Highly Nonlinear Wave Propagation in Elastic Woodpile Periodic Structures

E. Kim,[1] F. Li,[1] C. Chong,[2] G. Theocharis,[3] J. Yang,[1,*] and P. G. Kevrekidis[2]
[1]Aeronautics and Astronautics, University of Washington, Seattle, Washington 98195-2400, USA
[2]Department of Mathematics and Statistics, University of Massachusetts, Amherst, Massachusetts 01003-4515, USA
[3]Laboratoire d' Acoustique de l' Université du Maine, UMR-CNRS, 6613 Avenue Olivier Messiaen, 72085 Le Mans, France
(Received 30 April 2014; published 17 March 2015)

In the present work, we experimentally implement, numerically compute with, and theoretically analyze a configuration in the form of a single column woodpile periodic structure. Our main finding is that a Hertzian, locally resonant, woodpile lattice offers a test bed for the formation of genuinely traveling waves composed of a strongly localized solitary wave on top of a small amplitude oscillatory tail. This type of wave, called a nanopteron, is not only motivated theoretically and numerically, but is also visualized experimentally by means of a laser Doppler vibrometer. This system can also be useful for manipulating stress waves at will, for example, to achieve strong attenuation and modulation of high-amplitude impacts without relying on damping in the system.

DOI: 10.1103/PhysRevLett.114.118002 PACS numbers: 45.70.-n, 05.45.-a, 46.40.Cd

Introduction.—Granular crystals are rapidly becoming a popular vehicle for the theoretical study, numerical exploration, and experimental identification of a wide range of phenomena ranging from the near linear to the weakly or even highly nonlinear limit [1–4]. The relevant chains consist of assemblies of particles in one, two, and three dimensions inside a matrix (or a holder) in ordered, closely packed configurations. An especially appealing characteristic of such structures is the ability to tune their dynamic response by an applied static load. This may place the system in a near linear or weakly nonlinear regime, in the case of precompressed chains, or even in a highly nonlinear regime, in the absence of such a static load (often termed sonic vacuum, due to the vanishing sound speed in that case) [1]. It is exactly this dynamic tunability and the controllability of both the assembly and the measurement of these settings that has enabled a wide range of proposals for applications. Among others, we note shock and energy absorbing layers [5–7], acoustic lenses [8], acoustic diodes and switches [9,10], and sound scramblers [11].

While various geometries of building blocks have been reported (e.g., spherical, toroidal, or elliptical shapes), granular crystals in woodpile architectures, made of orthogonally stacked rods, are largely unexplored. This is in contrast to their electromagnetic counterpart—called woodpile photonic crystals—that successfully demonstrated their efficacy and versatility in manipulating electromagnetic waves [12,13]. Even existing studies on woodpile phononic crystals are limited primarily to their linear elastic responses [14–16], without addressing their nonlinear wave dynamics.

In this Letter, we show that periodic structures in woodpile configurations can be very useful in manipulating highly nonlinear stress waves at will, including potentially strong wave attenuation and spontaneous formation of novel traveling waves after an impact excitation. Arguably, the most fundamental waveform that arises in granular chains within the sonic vacuum is a solitary wave with a highly localized waveform [17–22]. Recently, other types of coherent traveling waves in granular chains, within the sonic vacuum, were predicted to exist: periodic traveling waves [20,23] and static or traveling breathers in granular chains including on-site potentials [24].

Here, we report experimental evidence of the existence of a new type of nonlocal solitary wave within the sonic vacuum. It consists of a highly localized solitary waveform on top of an extended, small-amplitude periodic tail, existing in granular chains with local resonators. Such a solution, satisfying all the other requirements of a solitary wave except that it asymptotes not to zero but to a small amplitude oscillation at infinity, has been long termed a nanopteron [25]. This nanopteron arises in numerous models including continuum [26–28] and discrete [29] dynamical systems. Some examples, like the ϕ^4 breather, have received considerable theoretical attention [26,30,31] and relevant reviews or books have summarized much of this nonlocal solitary wave activity [32,33]. Nevertheless, experimental studies of the nanopteron are extremely limited [28].

In what follows, we present the experimental setup of the woodpile lattice and a brief overview of its description via an effective discrete element model (DEM). In different regimes, we experimentally observe (i) the spontaneous formation and steady propagation of the nanopteron, (ii) the potential breathing of the solitary waves, i.e., modulation as they travel, or (iii) the decay of the solitary waves, which is due to the coupling to the internal resonant modes, rather than the damping of the system. All of the relevant features are corroborated by numerical computations, and some of the salient features are explained theoretically. We thus believe that this study provides a road map for further

exploration and analysis of highly nonlinear waves in a host of settings, including most notably granular chain models with the addition of an internal resonator on each node, a context that has recently been of considerable interest in its own right [34–38].

Experimental and theoretical setup.—Figure 1 illustrates the experimental setup of our 1D woodpile structure and the corresponding DEM. The chain is composed of orthogonally stacked cylindrical rods made of fused quartz (Young's modulus $E = 72$ GPa, Poisson's ratio $v = 0.17$, and density $\rho = 2200$ kg/m^3). We test three different rod lengths, [20, 40, 80] mm, while keeping their diameters identical to 5.0 mm. We excite the chain by striking the center of the uppermost rod with a 10-mm-diameter glass sphere. While we present in this Letter the results for a measured impact velocity of $V_0 = 1.97$ m/s, the effect of varying striker velocities can be found in the Supplemental Material [39]. We record the transmitted stress waves using a piezoelectric force sensor (PCB C02) placed at the bottom of the woodpile chain. To investigate the propagating waveforms along the path, we alter the number of stacked cylinders from 1 to N (total number of cylinders) and synchronize the signals with respect to the striker impact moment, which is detected by a small piezoelectric ceramic plate bonded on the surface of the top rod. A particular challenge within our setup concerns the experimental identification of the especially weak oscillations of the unit cells that are critical for our reported observation of the nanopteron. For this, we introduce a laser Doppler vibrometer (Polytec, OFV-505), which is mounted on an automatic sliding rail to detect localized vibrations of each rod in the resolution of 0.02 μm/s/Hz$^{1/2}$.

As suggested by Fig. 1(b), the dynamics of the woodpile lattice along the axis of the contacts can be effectively described by a system of nonlinear oscillators that are coupled to adjacent masses. Assuming the principal nodes (associated with the rods' axial motion) to have mass M and a coupling of β_c, and the internal resonators within the rods to have a coupling of k_1 and a mass of m_1, we propose the following generalized Hertzian DEM:

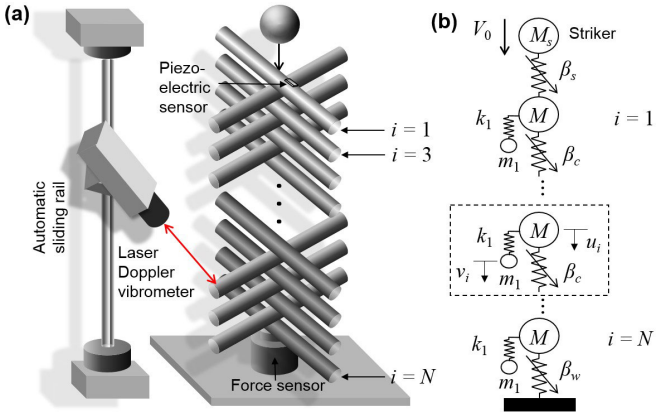

FIG. 1 (color online). Schematic of (a) experimental setup and (b) discrete element model; see text for details.

$$M\ddot{u}_i = \beta[u_{i-1} - u_i]_+^{3/2} - \beta[u_i - u_{i+1}]_+^{3/2} + k_1(v_i - u_i), \quad (1)$$

$$m_1\ddot{v}_i = k_1(u_i - v_i), \quad (2)$$

where u_i and v_i are the displacements of the i-th primary and auxiliary masses, and $[s]_+ = \max(s, 0)$, implying no tensile strength in the chain. This model allows us to describe longitudinal excitations along the axis of the contacts in the presence of internal vibration modes that can store energy in their own right.

The effective parameters m_1, M, and k_1 of this DEM description are determined via an optimization process based on the envelopes of propagating waves (see the Supplemental Material for further details [39]). Note that in Eq. (1), β assumes the value β_c within the chain, while it is β_s for the coupling of the striker to the first bead and β_w for the coupling of the last bead to the wall (cf. Fig. 1). In what follows, we will rescale the time $t \to t\sqrt{\beta_c/M}$ and the coupling $\kappa = k_1/\beta_c$ for the purposes of our analysis. The mass ratio is denoted by $\nu = m_1/M$.

Experimental observations, numerical corroboration, and theoretical analysis.—Figures 2(a) and 2(b) illustrate the comparison of the wave propagation in 1D woodpile lattices composed of 20 particles of 20 and 40 mm rods, respectively. Dashed red (solid black) curves represent the

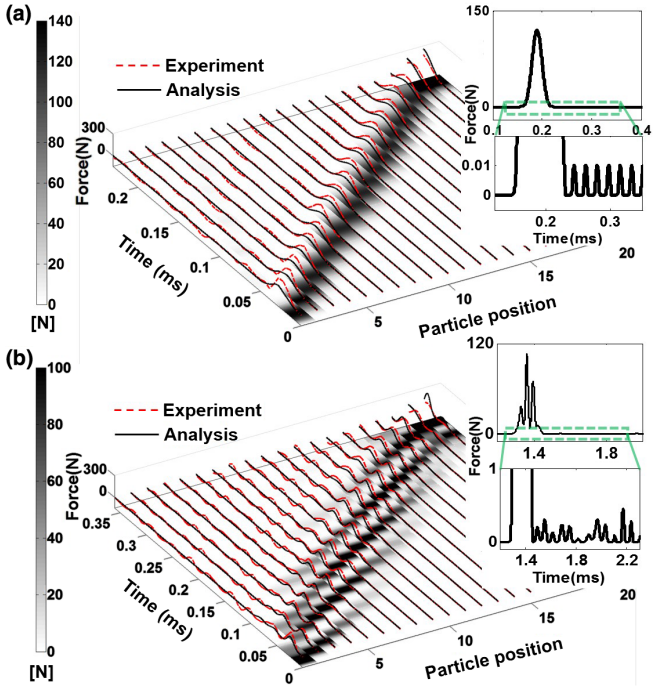

FIG. 2 (color online). Numerical (solid black) and experimental (dashed red) force profiles in space-time (measured in ms) in 1D woodpile crystals composed of (a) 20 mm and (b) 40 mm rods. The insets show the numerical magnified force profiles of nanoptera, while the colormap represents the magnitude of the contact force.

contact force profiles obtained by experiments (numerics). The numerical results are also shown in the underlying surface maps to ease visualization of wave modulation effects. In addition to the accurate representation of the experimental findings by the DEM, we can make a few further observations here. In the case of 20 mm rods, the striker rapidly settles into a solitary wave (in a way reminiscent of the standard granular chain [1,2]—however, with a significant difference, as we will see below). For the 40 mm case, a traveling breather appears to form in a pattern similar to numerical observations in Ref. [24]. This wave emerges after a transient period in which a primary wave experiences an exponential decay (which can be computed semianalytically, see the Supplemental Material [39]) and a secondary wave emerges due to the coupling with the resonators. However, a key feature shared by both traveling structures is the existence of a persistent form of background oscillation as seen in the insets of Fig. 2. We note that here the wake of the principal pulse has a constant amplitude tail. This feature, which has also been confirmed by means of simulations in considerably larger chains (as illustrated through suitable numerical experiments in the Supplemental Material [39]), is different from what is the case in the so-called Kawahara solitary waves, where the tail is decaying in amplitude away from the main wave shape [48]. It should also be mentioned that these weakly nonlocal solitary waves form even in the presence of dissipation although their features may be attenuated over time (again, we briefly discuss the relevant features in the Supplemental Material [39]). We now explore this nanopteronic waveform more quantitatively.

The surface maps in Figs. 3(a) and 3(b) show the analytical and experimental velocity profiles, respectively, of the tails of the observed waveforms that appear in a 40 particle chain of 20 mm rods. The traveling waves spontaneously become nanoptera by developing oscillatory patterns of velocity, which clearly follow the principal solitary wave (highlighted in red color). It should be noted that the velocities involved in the nanopteronic tails are approximately 3 orders of magnitude smaller than those of the solitary waves; yet, they can be accurately measured through the laser Doppler vibrometer. The frequency and wave number content of the nanopteronic tail can be obtained by conducting the fast Fourier transform (FFT) in time and space domains [shown in Figs. 3(c) and 3(d)]. The resonant frequency of the experimental data shown in Fig. 3(c) is 54.93 kHz, which is found to be directly connected to the relative motion of the two masses (the primary and the resonator ones), namely $\omega_0 = \sqrt{\kappa(1+1/\nu)}$ (55.45 kHz according to the DEM). For a traveling wave of speed c, the corresponding wave number in Fig. 3(d) is found to satisfy the relation $\omega_0 = ck_0$. In Fig. 3(d), we obtain $k_0 = 119\ \mathrm{m}^{-1}$ experimentally, which is in agreement with the value $k_0 = 120\ \mathrm{m}^{-1}$ obtained via the DEM (see the Supplemental Material for details [39]).

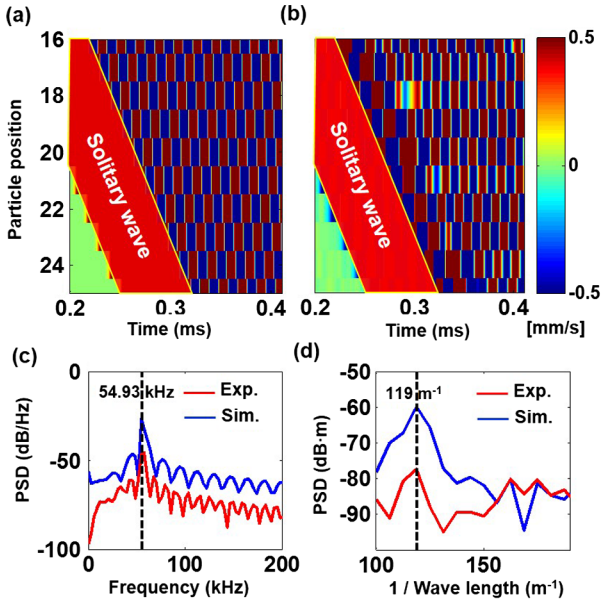

FIG. 3 (color online). (a) Numerical and (b) experimental velocity profiles of nanoptera formed in a 40 particle chain of 20 mm rods. (c) Frequency and (d) wave number contents of the tail constructed by the FFT of velocity profiles in specific time and space domains, respectively (particle spot $i = 24$ and time $t = 0.4$ ms).

We now theoretically justify this feature, namely the existence of the relative motion between the primary node and the resonator, in the nanopteronic tail of the observed wave structure. Setting up the so-called strains of the two fields $r_i = u_{i-1} - u_i$ and $s_i = v_{i-1} - v_i$, seeking traveling waves therein as $r_i(t) = R(i - ct) = R(\xi)$, $s_i = S(i - ct) = S(\xi)$, and then assuming that the Fourier transform $R(\xi) = \int_{-\infty}^{\infty} \hat{R}(k) e^{ik\xi} dk$ (and similarly for S) can be applied, leads from Eqs. (1) and (2) to

$$\hat{R} = \frac{1}{c^2}\mathrm{sinc}^2\left(\frac{k}{2}\right)\widehat{R^{3/2}} + \frac{\kappa}{k^2c^2}(\hat{R} - \hat{S}), \tag{3}$$

$$\hat{S} = \frac{\kappa}{\kappa - c^2k^2\nu}\hat{R}. \tag{4}$$

Substituting Eq. (4) into Eq. (3) and reshaping the relevant expression yields

$$\hat{R} = \left[\frac{1}{c^2}\mathrm{sinc}^2\left(\frac{k}{2}\right) + \frac{1}{c^4}\frac{\kappa}{k^2 - k_0^2}\mathrm{sinc}^2\left(\frac{k}{2}\right)\right]\hat{R^{3/2}}. \tag{5}$$

Recall that $\mathrm{sinc}\,(x) = \sin(x)/x$. Invoking the convolution theorem leads us to write

$$R(x) = K * R^{3/2} = \int_{-\infty}^{\infty} K(x - y)R^{3/2}(y)dy, \tag{6}$$

where $K(x) = \Lambda(x) + M(x)$, where $\Lambda(x) = (1/c^2)\max(1 - |x|, 0)$ and appears in the corresponding

calculation for the granular chain without internal resonators [19]. For $M(x)$ we find

$$(2c^4k_0^3/\kappa)M(x) = |1-x|[\mathrm{sinc}(k_0(1-x)) - k_0] - 2|x|[\mathrm{sinc}(k_0x) - k_0] + |x+1|[\mathrm{sinc}(k_0(x+1)) - k_0]. \quad (7)$$

Thus, the sinusoidal dependence with the periodicity dictated by k_0 within $M(x)$ is directly responsible for the formation of the nanopteronic tails, cf. also the resonant term in the Fourier space expression of Eq. (5). In the granular chain without the resonators, the presence of solely the Λ term in Eq. (5) produces a monotonically decaying solitary wave according to a double exponential law [19,21]. Here, the presence of the sinusoidal terms within $M(x)$ justifies the form of the nanopteron, where the localized central wave is supported against the backdrop of linear relative vibrations between each node and its corresponding resonator.

Finally, it should be noted that the present setup provides numerous additional opportunities for a wide range of studies within this class of models. One such study consists of modifying the rod length. For example, the experimental and numerical results for 80 mm rods are shown in Fig. 4. In this case, the DEM needs to account for two internal resonant modes within the rod and hence two resonators (v_i, w_i) are attached to each principal node of the chain (u_i). As a result, we observe that in this case, the large-amplitude striker impact drastically decays through an effective excitation of the internal resonant modes, which disperse the energy in both the temporal and the spatial domain. The inset of Fig. 4 depicts the overlapped profiles of nonlinear waves obtained from various particle positions, which evidently indicate the decaying trend of the propagating waves due to the coupling to the resonators. This wave attenuation suggests that the woodpile periodic structure could be used as an efficient impact mitigator without relying on damping in the system. We should note here that

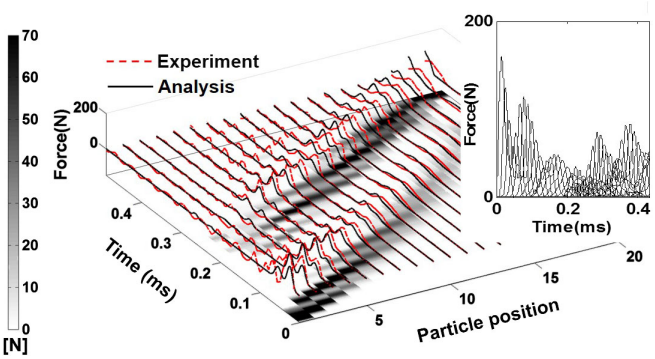

FIG. 4 (color online). Experimental and numerical space-time wave modulation results in woodpile crystals composed of 80 mm rods.

although in this exposition we have highlighted some of the salient features of the model, numerous additional details including the quantitative nature of the agreement between theory, numerics, and experiment are provided in the Supplemental Material (see, e.g., Fig. 8 therein) [39].

Conclusions and future challenges.—In the present work, we have offered a prototypical example of a woodpile granular crystal, consisting of a chain of orthogonally stacked cylindrical rods. In addition to developing the experimental techniques enabling a distributed space-time sensing of the chain, we have provided a theoretical discrete element model that captures the fundamental experimental characteristics of the system, while generalizing the standard Hertzian chain via the inclusion of at least one or modularly more internal mode resonators. We have seen that this inclusion provides the possibility for a potential breathing traveling wave or even decay of the initial strong impulse. More importantly, the relative motion between each node and its corresponding resonator provides the linear mode, which constitutes the background for the formation of a weakly nonlocal solitary wave, i.e., a nanopteron. Despite the small magnitude of the tails of the nanoptera (differing by 3 orders of magnitude with respect to the principal wave), we were able to experimentally observe and compute these tails and to theoretically account for the wave number or frequency of their periodicity.

This study leads to a number of topics for potential future work. From a rigorous mathematical perspective, proving the existence of the nanopteron provides a novel set of challenges. At the discrete element model level, quantifying the properties of the system in the case of one or more resonators by detailing the interplay between principal and secondary waves or the role of parametric variations (such as tuning the resonant frequency of the coupling between unit cells, etc.) would be of particular interest. It is also relevant to point out that our numerically or experimentally observed nanoptera have a tail only on one side (i.e., are "one-sided" nanoptera), while the typical examples previously known have tails on both sides. Understanding when one-sided versus two-sided installments of such coherent structures may arise could be of particular interest for future work. In the same vein, considering the results of collisions of two such (e.g., counterpropagating) waves could also shed light on the robustness of such one-sided nanoptera, as well as potentially lead to the formation of two-sided variants thereof. Finally, several questions naturally emerge in experimental investigations. These include examining the problem in the presence of precompression and its generalization to higher dimensional settings. From a practical perspective, this woodpile structure can offer a new way to modulate, localize, or mitigate external impacts for engineering devices and associated applications.

We thank C. Daraio, D. Khatri, and D. Frantzeskakis for helpful discussions. J. Y. and P. G. K acknowledge the

support of NSF (Grants No. CMMI-1414748, No. CMMI-1000337, and No. DMS-1312856), AFOSR (Grant No. FA9550-12-1-0332), and ONR (Grant No. N000141410388). G. T. acknowledges financial support from FP7-CIG (Project 618322 ComGranSol).

*Corresponding author.
jkyang@aa.washington.edu

[1] V. F. Nesterenko, *Dynamics of Heterogeneous Materials* (Springer-Verlag, New York, 2001), Chap. 1.
[2] S. Sen, J. Hong, J. Bang, E. Avalosa, and R. Doney, Phys. Rep. **462**, 21 (2008).
[3] P. G. Kevrekidis, IMA J. Appl. Math. **76**, 389 (2011).
[4] G. Theocharis, N. Boechler, and C. Daraio, in *Acoustic Metamaterials and Phononic Crystals*, edited by P. A. Deymier (Springer, New York, 2013), Chap. 7.
[5] C. Daraio, V. F. Nesterenko, E. B. Herbold, and S. Jin, Phys. Rev. Lett. **96**, 058002 (2006).
[6] J. Hong, Phys. Rev. Lett. **94**, 108001 (2005).
[7] R. Doney and S. Sen, Phys. Rev. Lett. **97**, 155502 (2006).
[8] A. Spadoni and C. Daraio, Proc. Natl. Acad. Sci. U.S.A. **107**, 7230 (2010).
[9] N. Boechler, G. Theocharis, and C. Daraio, Nat. Mater. **10**, 665 (2011).
[10] F. Li, P. Anzel, J. Yang, P. G. Kevrekidis, and C. Daraio, Nat. Commun. **5**, 5311 (2014).
[11] V. F. Nesterenko, C. Daraio, E. B. Herbold, and S. Jin, Phys. Rev. Lett. **95**, 158702 (2005).
[12] A. Feigel, M. Veinger, B. Sfez, A. Arsh, M. Klebanov, and V. Lyubin, Appl. Phys. Lett. **83**, 4480 (2003).
[13] H. Liu, J. Yao, D. Xu, and P. Wang, Opt. Express **15**, 695 (2007).
[14] H. Jiang, Y. Wang, M. Zhang, Y. Hu, D. Lan, Y. Zhang, and B. Wei, Appl. Phys. Lett. **95**, 104101 (2009).
[15] L. Y. Wu and L. W. Chen, J. Phys. D **44**, 045402 (2011).
[16] E. Kim and J. Yang, J. Mech. Phys. Solids **71**, 33 (2014).
[17] V. F. Nesterenko, J. Appl. Mech. Tech. Phys. **24**, 733 (1984).
[18] R. S. MacKay, Phys. Lett. A **251**, 191 (1999).
[19] J. M. English and R. L. Pego, Proc. Am. Math. Soc. **133**, 1763 (2005).
[20] Y. Starosvetsky and A. F. Vakakis, Phys. Rev. E **82**, 026603 (2010).
[21] A. Stefanov and P. Kevrekidis, Nonlinearity **26**, 539 (2013).
[22] A. Chatterjee, Phys. Rev. E **59**, 5912 (1999).
[23] G. James, J. Nonlinear Sci. **22**, 813 (2012).
[24] G. James, P. G. Kevrekidis, and J. Cuevas, Physica (Amsterdam) **251D**, 39 (2013).
[25] J. P. Boyd, in *Nonlinear Topics in Ocean Physics: Proceedings of the Fermi School*, edited by A. R. Osborne and L. Bergamasco (Amsterdam: North-Holland, 1991), pp. 51–97.
[26] H. Segur and M. D. Kruskal, Phys. Rev. Lett. **58**, 747 (1987).
[27] A. V. Buryak, Phys. Rev. E **52**, 1156 (1995); N. N. Akhmediev, A. V. Buryak, Opt. Commun. **121**, 109 (1995).
[28] T. Akylas and R. Grimshaw, J. Fluid Mech. **242**, 279 (1992); An interesting feature in this particular case is that it consists of a single figure based on the earlier experimental work of D. Farmer and J. Smith, Deep-Sea Res. **27**, 239 (1980), which was provided to T. Akylas and R. Grimshaw by Dr. Farmer.
[29] G. Iooss and G. James, Chaos **15**, 015113 (2005).
[30] J. P. Boyd, Nonlinearity **3**, 177 (1990).
[31] N. Lu, J. Diff. Equ. **256**, 745 (2014).
[32] J. Boyd, *Weakly Nonlocal Solitary Waves and Beyond-All-Orders Asymptotics* (Kluwer, Amsterdam, 1998).
[33] J. P. Boyd, Acta Appl. Math. **56**, 1 (1999).
[34] B. S. Lazarov and J. S. Jensen, Int. J. Nonlinear Mech. **42**, 1186 (2007).
[35] P. G. Kevrekidis, A. Vainchtein, M. Serra Garcia, and C. Daraio, Phys. Rev. E **87**, 042911 (2013).
[36] L. Bonanomi, G. Theocharis, and C. Daraio, arXiv: 1403.1052.
[37] G. Gantzounis, M. Serra-Garcia, K. Homma, J. M. Mendoza, and C. Daraio, J. Appl. Phys. **114**, 093514 (2013).
[38] K. Vorotnikov, Y. Starosvetsky, G. Theocharis, and P. G. Kevrekidis (to be published).
[39] See Supplemental Material at http://link.aps.org/supplemental/10.1103/PhysRevLett.114.118002, which includes Refs. [40–47] for experimental setup, the precise selection of the DEM parameters, and the effects of damping and excitation amplitude on the nanopteron.
[40] C. Coste, E. Falcon, and S. Fauve, Phys. Rev. E **56**, 6104 (1997).
[41] S. Job, F. Melo, A. Sokolow, and S. Sen, Granular Matter **10**, 13 (2007).
[42] Y. Tsuji, T. Tanaka, and T. Ishida, Powder Technol. **71**, 239 (1992).
[43] G. Friesecke and J. A. D. Wattis, Commun. Math. Phys. **161**, 391 (1994).
[44] A. Stefanov and P. G. Kevrekidis, J. Nonlinear Sci. **22**, 327 (2012).
[45] Y. Starosvetsky, Phys. Rev. E **85**, 051306 (2012).
[46] K. Lindenberg, U. Harbola, H. Romero, and A. Rosas, AIP Conf. Proc. **1339**, 97 (2011).
[47] K. Ahnert and A. Pikovsky, Phys. Rev. E **79**, 026209 (2009).
[48] T. Kawahara, J. Phys. Soc. Jpn. **33**, 260 (1972); see also C. I. Christov, G. A. Maugin, and M. G. Velarde, Phys. Rev. E **54**, 3621 (1996).